Molecular Systems Biology 6; Article number 444; doi:10.1038/msb.2010.99
**Citation:** ***Molecular Systems Biology*** **6:444**

www.molecularsystemsbiology.com

molecular systems biology

**REPORT**

# A tunable dual-promoter integrator for targeting of cancer cells

**Lior Nissim and Roy H Bar-Ziv***

Department of Materials and Interfaces, The Weizmann Institute of Science, Rehovot, Israel
* Corresponding author. Department of Materials and Interfaces, The Weizmann Institute of Science, Herzel Street, Rehovot 76100, Israel. Tel.: +972 8 9342069; Fax: +972 8 9344138; E-mail: Roy.Bar-ziv@weizmann.ac.il

Received 28.7.10; accepted 25.10.10

**Precise discrimination between similar cellular states is essential for autonomous decision-making scenarios, such as *in vivo* targeting of diseased cells. Discrimination could be achieved by delivering an effector gene expressed under a highly active context-specific promoter. Yet, a single-promoter approach has linear response and offers limited control of specificity and efficacy. Here, we constructed a dual-promoter integrator, which expresses an effector gene only when the combined activity of two internal input promoters is high. A tunable response provides flexibility in choosing promoter inputs and effector gene output. Experiments using one premalignant and four cancer cell lines, over a wide range of promoter activities, revealed a digital-like response of input amplification following a sharp activation threshold. The response function is cell dependent with its overall magnitude increasing with degree of malignancy. The tunable digital-like response provides robustness, acts to remove input noise minimizing false-positive identification of cell states, and improves targeting precision and efficacy.**
*Molecular Systems Biology* **6**: 444; published online 21 December 2010; doi:10.1038/msb.2010.99
*Subject Categories:* synthetic biology
*Keywords:* cancer; gene therapy; signal integration; synthetic biology; systems biology



## Introduction

### A dual-promoter integrator approach

Providing cells with autonomous, decision-making genetic systems to diagnose and intervene with their own fate would advance our ability to manipulate cell populations based on their expression patterns; this could be used for example in targeting diseased tissues, while leaving normal cells intact. Autonomous targeting of unique expression patterns from among a background of similar ones requires systems that respond to internal cellular indicators, such as promoters, with sufficient precision to uniquely discern the state of interest. Yet, decision-making based on a single element inherently suffers from noise, lack of specificity, and false-positive identification. Integrating two indicators can qualitatively improve the precision: the probability $p$ of incorrectly identifying a cell state based on a single indicator is reduced to $p^2$ when combining two independent parameters. In nature, synergy and integration of two inputs enhances the fidelity versus a single one, induces sharpness of response, and confers robustness to biochemical processes. For example, (i) genetic switches and signaling cascades are commonly triggered by protein dimers rather than monomers (Ptashne, 1988; Heldin, 1995; Hoffmann *et al*, 2006), (ii) the translation of the genetic material is iterated by proofreading steps to increase precision (Hopfield, 1974), and (iii) cell proliferation requires integration of both proliferative signals and anti-apoptotic ones (Harrington *et al*, 1994; Evan and Littlewood, 1998; Mebratu and Tesfaigzi, 2009).

Expression-based targeting has been used in gene therapy of cancer. A plasmid or viral vector encoding a cytotoxic effector gene regulated by a cancer-specific promoter is delivered into the cells, ideally killing only cancer cells in which the targeted promoter is highly active (Dachs *et al*, 1997; Nettelbeck, 2008; Dong and Nor, 2009; Dorer and Nettelbeck, 2009). But while the targeted promoter might be abnormally active only in cancer cells of a certain tissue, it may be expressed in a normal tissue of a different origin (Kim *et al*, 1993; Hernandez and Thompson, 2004; Ohana *et al*, 2004; Peng *et al*, 2005). Therefore, the likelihood of undesired activation of the killer gene in healthy cells increases with the diversity of tissues exposed to the delivery system. A dual-promoter targeting approach has been used in oncolytic viruses by combining a cell cycle-specific promoter with a cancer-specific one

(Ryan *et al*, 2004; Li *et al*, 2005), and its activity and specificity was demonstrated in a melanoma model using a modified mammalian two-hybrid system encoded on plasmids (Jerome and Muller, 1998, 2001). Yet, the design principles governing the responses of dual-promoter systems have so far not been experimentally characterized, precluding further progress. In this study, we used a modular dual-promoter expression integrator (DPI) and measured its input–output response function (I/O) over a wide promoter activity range and in a number of cell lines. This I/O measurement is our central methodological result, with characterization of amplification, sharpness of response, and threshold of minimal inputs for significant output.

## DPI design

Internal signals could be artificially combined to yield a single biological output (Lim, 2010), for example, as demonstrated in bacteria (Anderson *et al*, 2007; Callura *et al*, 2010), yeast (Nissim *et al*, 2007), and mammalian cells (Deans *et al*, 2007; Tigges and Fussenegger, 2009; Leisner *et al*, 2010). We have previously designed a DPI to operate in yeast that acts autonomously as a logical AND gate on two cellular metabolic promoters, expressing a killer (or reporter) gene only when the two promoters are both active beyond a minimal threshold (Nissim *et al*, 2007). The current DPI is based on a modification of the mammalian two-hybrid system (Betzi *et al*, 2007), and includes three genes and their promoters, encoded on plasmids (Box 1 and Supplementary information). To control expression of the output gene, two fusion proteins are regulated by two duplicates of native promoters whose concurrent activity was chosen as a marker of a transformed phenotype. The two fusion proteins are thus expressed in proportion to the activity of the promoters chosen. The fusion proteins must bind to form a transcriptional complex to enable expression of the output gene. The design utilizes the bacterial DocS fused to the viral VP16 transcription activation domain, and the bacterial Coh2 fused to Yeast GAL4 DNA binding domain, in which DocS and Coh2 bind with very high affinity (Barak *et al*, 2005). Together, the fusion proteins form a transcription complex, capable of activating the expression of an output gene regulated by its own synthetic promoter (containing five GAL4 binding sites). The output is either the luciferase reporter gene for calibration of the system, or, to induce cell death, the herpes simplex virus type-1 thymidine kinase (TK1), which is cytotoxic in the presence of nucleotide analogs such as E-5-2-bromovinyl-2′-deoxyuridine (BVDU) or ganciclovir (GCV; Wera *et al*, 1999).

**Box 1 DPI design**

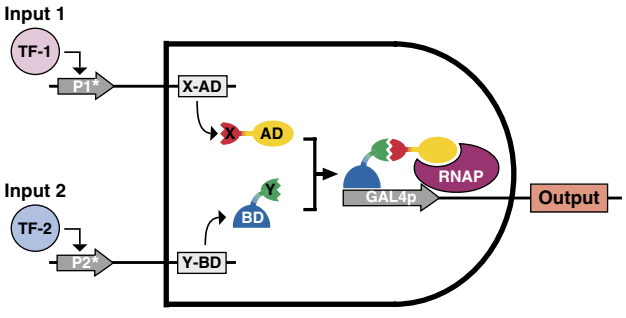


TF1 and TF2 are upstream transcription factors determining expression of two native promoters (P1 and P2, not shown). P1* and P2* are copies of P1 and P2, containing the promoter region 600–1000 bp upstream of the ATG, delivered on two plasmids. DocS-AD (denoted X-AD) and Coh2-BD (denoted Y-BD) are fusion proteins regulated by P1* and P2*: DocS (denoted X) and Coh2 (denoted Y) dimerize tightly; AD=viral VP16 transcription activation domain; BD=yeast GAL4 binding domain. The transcriptional complex activates a synthetic yeast GAL4 promoter, regulating output gene expression (delivered on a third plasmid). Output=luciferase reporter or TK1 killer genes.

## Choice of cell lines and promoters

To investigate the properties of the dual versus single-promoter approach in discriminating between cells with similar expression patterns, we chose two pairs of closely related cell lines: premalignant and tumor WI38-derived lung fibroblasts, and two close derivatives of the HCT116 human colorectal tumor line. The premalignant WI38/T/NEO cells (Milyavsky *et al*, 2005; Tabach *et al*, 2005), together with the p53 knockdown WI38/T3 tumor cells overexpressing H-Ras$^{V12}$, were previously generated as an *in vitro* model of lung cancer development (Milyavsky *et al*, 2003; Buganim *et al*, 2010). HCT116+/+ (p53 expressing) and HCT116−/− (p53 deficient) are commonly used cancer cell lines (Liu *et al*, 2007), which have very similar expression patterns and many overexpressed genes in common with the T3 cell line. Normal cells were not used for two reasons: (i) premalignant cells are already partially transformed and have expression patterns more similar to those of tumor cells than do normal ones, and hence their discrimination posed a greater challenge; (ii) normal cells have low transfection efficiency and are difficult to maintain in culture.

Optimally, the dual-promoter approach requires promoters that are highly active in cancer cells and whose mutual activity is improbable in normal ones. To map the I/O, we chose cancer-related promoters exhibiting a wide range of activities in the different cell lines. Three promoters were chosen as candidates to discriminate tumor cells from premalignant ones, as they are known to be highly active in HCT116 and T3 cells, but not in T/NEO: the chromatin structural protein histone-H2A1 promoter (Rogakou *et al*, 1998); the synovial sarcoma X-breakpoint protein-1 SSX1 promoter (Gure *et al*, 1997); and the inflammatory chemokine CXCL1 promoter (Wang *et al*, 2006). Finally, the CDK4/6 kinase regulator CyclinD1 promoter was used as a negative control, as it has very low activity in all four cell lines (Morgan, 1997). These promoters were cloned as inputs for single-promoter and DPI vectors using sequences that are 600–1000 bp upstream of the ATG (including the 5′ UTR) of each native gene. These synthetic promoters are regulated by the same endogenous transcription factors associated with the native promoters. Yet, they might not include upstream regulatory elements, and therefore might exhibit somewhat different activities than native promoters. Hence, the I/O must be measured within context of the DPI.

## Results and Discussion

### The I/O of a DPI in cancer cells

To map the I/O of the DPI, we first measured its inputs using firefly luciferase, separately expressed under each promoter in all four cell lines (Figure 1A, single rows). The data were normalized to the transfection efficiency, which was measured independently (see Materials and methods). In the premalignant T/NEO cells, the overall activity of all four promoters was low (10–100 counts per sec, CPS), whereas in the three cancer cells, the activity range of all promoters was high (172–1073 CPS), except for the inactive CyclinD1 used as the negative control (66–177 CPS).

We next measured the DPI luciferase expression using all $4 \times 4$ promoter pairs as inputs, plotting output as a function of promoter identity (Figure 1A) and activity (Figure 1B). In T/NEO cells, all promoter pairs gave low output (12–157 CPS), consistent with low input values. In contrast, in the three cancer lines, the DPI showed a clear hallmark of digital AND logic: (i) Threshold: the DPI output remained low (14–40 CPS) when one of the inputs was the inactive CyclinD1, irrespective of the activity level of the second input promoter. (ii) Sharpness: a 3D plot of the I/O irrespective of promoter identity reveals a significant step-like response in all cancer cell lines, but not in T/NEO (Figure 1B). (iii) Amplification: in T3 cells the input values were roughly equal to the output, yet they were amplified approximately 10-fold in HCT116+/+ and HCT116−/− cells (up to 3000 CPS); the response saturated at a maximal value for SSX1–SSX1, beyond which some attenuation was observed, for example, with H2A1–H2A1. The overall enhancement of the I/O with progressive tumorigenesis from T/NEO to T3, HCT116+/+, and HCT116−/− is expected, as malignant transformation also

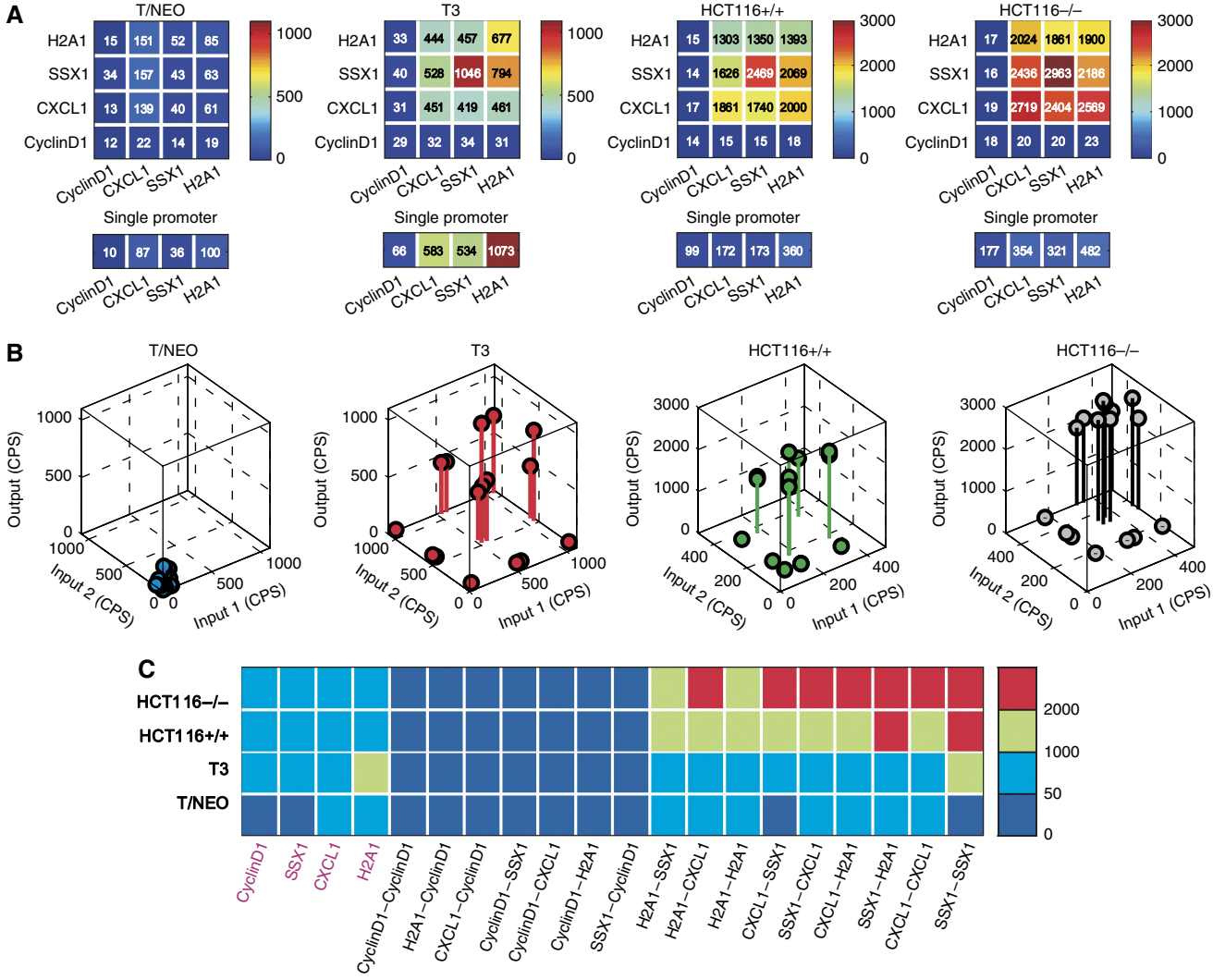


**Figure 1** I/O response function and threshold analysis. (**A**) 'Heat maps' of luciferase expression levels (actual values are indicated inside each entry) using single and dual input promoters in WI38-T/NEO, WI38-T3, HCT116+/+, and HCT116−/− cells, as indicated (rows=P1, columns=P2). STDEV for all samples are <15% of the indicated values. (**B**) The I/O relationship in terms of promoter pair activity irrespective of their identity in WI38-T/NEO, WI38-T3, HCT116+/+, and HCT116−/− cell lines. (**C**) Map of targeting options. The DPI promoter pair inputs are sorted in ascending order of luciferase output averaged over all four cell lines from left to right, and similarly for single promoters (left columns labeled in purple). The inputs and outputs were annotated according to a predetermined threshold: up to 50 CPS (blue), 50–1000 CPS (azure), 1000–2000 CPS (green), and above 2000 (red).

results in enhanced protein synthesis machinery (Caraglia *et al*, 2000; Boon *et al*, 2001). In all cell lines the output measured in control samples, in which one of the DPI plasmids was absent, was lower than 25 CPS (results not shown). As a digital device, the DPI is protected against noise at its inputs (signal restoration), which confers robustness to its activity. The I/O provides a unique signature for each cell line, thereby forming a basis for discriminative targeting.

To learn how the I/O translates into discriminative targeting of cells, and to define optimal choices of promoters and an effector gene, we must take in account that cell fate is dependent on effector concentration and potency. For example, the cellular concentration of diphtheria-toxin α-chain required for cell death is known to be extremely low (Yamaizumi *et al*, 1978). In contrast, TK1 causes cell death at a higher cellular concentration (Patil *et al*, 2000). Hence, to explore the susceptibility of cells to targeting, we assumed that the luciferase reading is proportional to the concentration of the effector gene product, and then defined varying threshold values (in luciferase CPS) above which cell fate is presumably affected (Figure 1C). The input entries were sorted by ascending order of the DPI luciferase output averaged over all cell lines, and outputs were represented in blue (up to 50 CPS), azure (50–1000 CPS), green (1000–2000 CPS), or red (above 2000 CPS). The resulting threshold pattern simulated a range of possible effector gene potencies for all cells, including both single- and dual-promoter entries, highlighting available targeting options.

The DPI output was below 50 CPS in all cell lines when one of the inputs was the negative control promoter, CyclinD1, demonstrating the lack of false-positive targeting, which for the case of killer gene activation becomes increasingly important with the numbers of cell types that must be protected. As the threshold value increases, we notice that (i) using the DPI enables greater choice of input promoters compared with a single-promoter approach, a feature which is expected to maintain discrimination under scenarios involving numerous cell types and diverse transcription patterns; (ii) at high threshold ($>1000$ CPS), the single-promoter approach can hardly be used for targeting, and therefore weakly active effector genes could be used only with the dual-promoter strategy, due to the I/O amplification provided by the DPI; (iii) some targeting patterns (for example, targeting only HCT116 but not WI38 cells) are possible only with the DPI, while at low threshold, some discrimination options can be obtained only with a single promoter. Therefore, the DPI provides improved robustness, as well as more flexibility in choosing promoter inputs and an effector gene for discrimination.

## Targeting cancer cells by a DPI

We next replaced luciferase with the TK1 killer gene to assess cell fate determination by the DPI. The transfection efficiency was estimated in each sample separately 48 h after transfection. The cells were co-transfected with an auxiliary plasmid expressing GFP under a stable promoter (pCMV-GFP; Materials and methods), and total GFP expression per sample was measured. Only then were the substrates for TK1 (GCV or BVDU) added. To exclude the effect of transfection-related cytotoxicity from TK1-induced cell death, the cell density was normalized to that of a negative control sample, namely, cells expressing luciferase output instead of TK1 under a DPI (separately for each cell line).

TK1 viability assays in T/NEO and T3 cells using GNC as substrate showed at most 20% transfection efficiency (determined by the percent of GFP-positive cells 48 h following transfection). In T/NEO, no targeted cell death could be observed beyond considerable non-specific transfection-induced growth arrest and cytotoxicity (Supplementary Figure S1). Yet, in T3 cells, significant variations in cell density were observed, suggesting specific targeting, despite some non-specific cytotoxic death as well (Figure 2A and B). Single-promoter TK1 activation with CXCL1, SSX1, and H2A1 led to nearly 100% cell death and even the inactive CyclinD1 promoter caused 80% death, suggesting a very low threshold for TK1 activation in T3. However, dual-promoter targeting exhibited up to twofold reduction of the background level of cell death with CyclinD1 as input (44–62%), and 67–88% death with two highly active input promoters (CXCL1, SSX1, and H2A1). The overall response of T3 cells to TK1 targeting retained the luciferase I/O AND-gate pattern. We note that T3 cell death was higher than expected based on the maximal observed transfection rate of 20%. This is likely due to a bystander effect of TK1 activity, which is mediated by cell–cell transfer of phosphorylated GCV via cellular gap junctions (Bi *et al*, 1993; Touraine *et al*, 1998). HCT116 cells showed TK1-independent sensitivity to GNC and BVDU, and hence could not be tested for targeting by TK1 (results not shown).

To further investigate targeting by DPI, circumventing the problems of transfection efficiency and non-specific cytotoxicity, we used the malignant human embryonic kidney cell line, HEK-293T, known for high transfection efficiency and wide dynamic range of expression. In HEK-293T cells, the range of CyclinD1, CXCL1, SSX1, and H2A1 promoter activity extended from 249 to 19126 CPS, as compared with 10–1073 CPS in the other cell lines (Figure 2C). As with other cells, SSX1 and H2A1 were highly active, yet both CXCL1 and CyclinD1 were inactive; we therefore used only CXCL1 as negative control. The dual-promoter I/O had the same AND-gate characteristics of sharpness of response, threshold and amplification up to ~12-fold.

Subsequently, we subjected HEK-293T cells to DPI targeting by TK1, but used BVDU as the substrate instead of GNC due to TK1-independent cytotoxicity of the latter (data not shown). In contrast to WI38 cells, the transfection efficiency of HEK-293T was essentially 100%. For single promoter, TK1 expression cell death was 60% with CXCL1 and nearly 100% with SSX1 and H2A1 promoters (Figure 2D and E). Under DPI targeting, cell death dropped to an average of 30% when one of the input promoters was inactive (CXCL1), and increased to nearly 100% when both input promoters were highly active. Luciferase outputs of 449–6143 CPS were sufficient to cause cell death of 23–42% (all samples with CXCL1 as one of the inputs). Therefore, the onset for TK1-induced cell death in HEK-293T corresponds to luciferase expression of hundreds to several thousand CPS. These results suggest that the sensitivity of HEK-293T cells to TK1 activity with BVDU is significantly lower than that of T3 cells to TK1 with GNC. Finally, the high background death (when at least one of the input promoters is inactive) in both T3 and HEK-293T suggests that reduced sensitivity may be required to improve targeting fidelity.

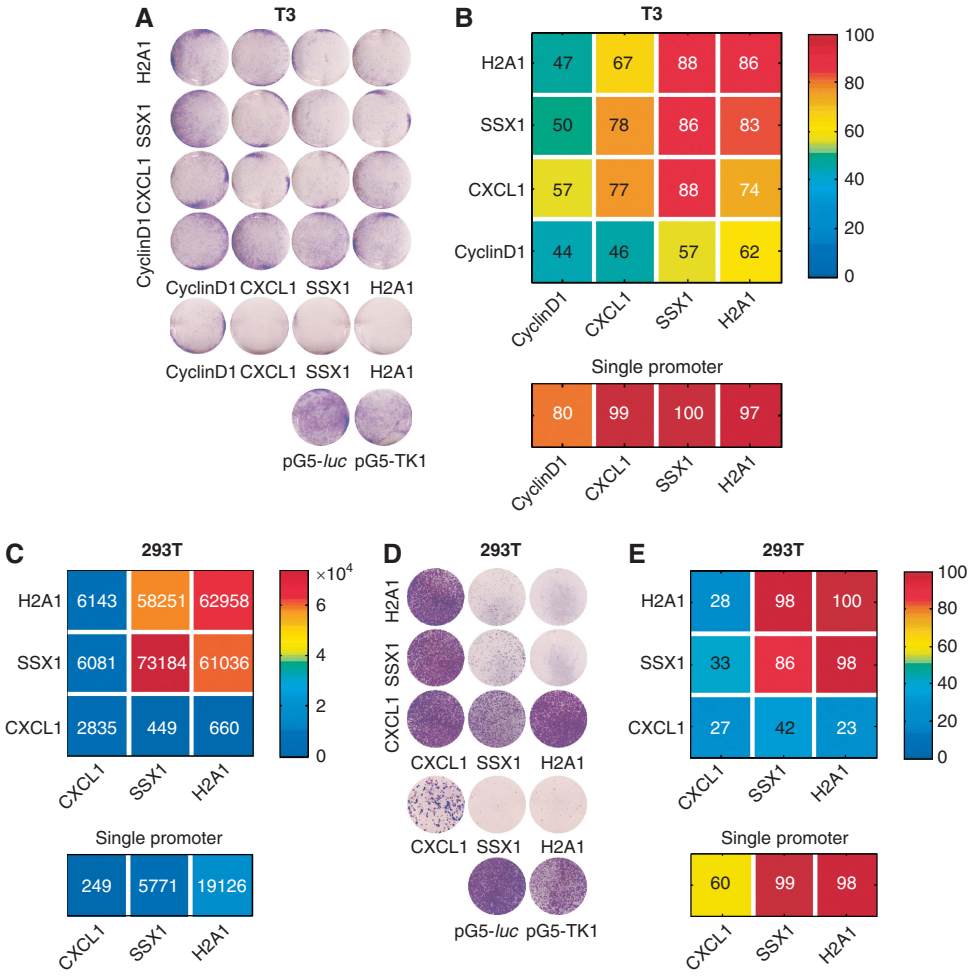


**Figure 2** Targeting of cells by the TK1 killer gene. (**A**) Cell death in WI38-T3 cells as determined by cell density using crystal violet staining (intense staining indicates viable samples). DPI promoter entries (top 4 × 4 matrix), single promoter (middle row), and negative controls of luciferase (or TK1) expressed under a GAL4 promoter using pG5-*luc* and pG5-TK1 plasmids solely (see Materials and methods). (**B**) Corresponding 'heat maps' of TK1-induced cell death percentage. STDEV for all samples are <20% of the indicated values. (**C**) Heat map of DPI I/O using luciferase activity in HEK-293T cells with dual- and single-promoter entries as indicated. STDEV for all samples are <15% of the indicated values. (**D**, **E**) Cell death and corresponding heat map under TK1 expression in HEK-293T cells, as in (A, B). STDEV for all samples are <20% of the indicated values.

## Tunable DPI response

To enhance the fidelity of cell-state discrimination, the DPI response strength must be tunable. For example, a highly responsive DPI might cause detrimental false-positive targeting of normal cells, as even weak promoter activity would suffice to trigger cell death when a potent effector gene is used. Weakening the DPI response would enable the use of promoters that are somewhat active in normal cells, as long as they are extremely active in abnormal ones, thereby removing the constraint of using only promoters that are completely inactive in normal cells and highly active in cancerous ones. Conversely, strengthening the DPI response would enable using weak promoters or relatively inefficient effector genes.

To weaken the response and shift the minimal threshold of the DPI toward higher input values, we replaced the wild-type DocS with a mutant derivative, DocS15 (D7/39/50A), which has a weaker interaction with Coh2, or with an even more weakly binding mutant, DocS102 (D18/15A; Karpol *et al*, 2008). The resulting DPI luciferase expression was demonstrated in HEK-293T cells due to their wide I/O dynamic range. As expected, the overall DPI output (measured by luciferase activity) was lower by roughly 10-fold with *DocS15*, and by 30-fold with *DocS102* relative to wild-type DocS (Figure 3). The salient feature of the modified DPI is that its output is very low for promoter input pairs for which at least one is inactive, resulting in a significantly reduced false-positive identification, and presumably, less background cytotoxicity. This comes at the expense of lower output for two active promoters.

## Conclusions

The assumption that 'two is better than one' was used here to provide simple design principle for expression-based targeting, with improved precision over single-promoter approaches. The I/O of the DPI (Figure 1A and B) is our central

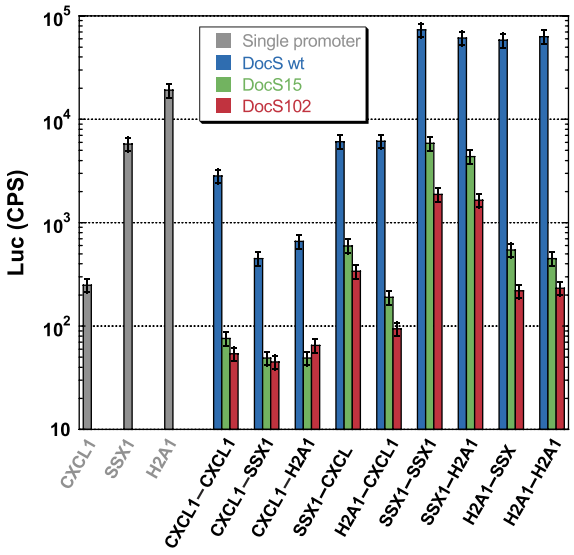


**Figure 3** Tuning the response of the DPI. The DPI I/O in HEK-293T cells measured with luciferase for three synthetic protein pairs (Box 1): DocS-WT/Coh2 (blue) and the more weakly binding pairs *DocS15*/Coh2 (green) and *Doc102*/Coh2 (red); single (gray bars) and dual-promoter entries are indicated.

result; the DPI exhibits a digital-like response, input amplification, and sharp threshold, which provide robustness and reduction of false-positive targeting of cell states, particularly important for targeting of cancer cells in cell populations with diverse promoter activities. Threshold analysis of the I/O using a reporter gene provides a basis for optimal choice of effector gene potency and promoter pairs (Figure 1C). The choice of synthetic proteins forming the DPI endows flexibility. Weakly binding proteins may be chosen for: (i) input promoters that are expressed at low levels in normal cells, but are significantly more active in cancer cells; or (ii) the use of potent effector genes, while maintaining acceptable levels of false-positive discrimination of normal cells. Conversely, strongly binding proteins are suitable for less potent effector genes and for picking up weak cancer-specific promoters, thereby enhancing the efficacy of targeting.

The DPI could be adapted to capture transient dual-promoter coincidence by reducing the lifetime of the synthetic proteins comprising the AND gate, using appropriate degradation fusion tags (Li *et al*, 1998). Similarly to two-hybrid systems used to unravel unknown protein–protein interactions, the DPI approach could be used, as well, to discover novel correlations between promoter pairs by screening promoter libraries. The use of *in vivo* imaging (IVIS) (Zhang *et al*, 2003) to measure promoter activity can be extended to measure dual-promoter correlations. Finally, identification of potential optimal promoter pairs for expression-targeted therapy can be achieved by replacing the killer gene with a helper gene to screen *in vitro* for promoter pairs that confer survival to cancer cells but not to normal ones.

Finally, viral delivery may be required for *in vivo* targeting, and proper function of a DPI requires the inclusion of three independently regulated promoter-gene modules on a single virus. DNA viruses, such as adenoviruses and HSV-1, could be used to deliver roughly up to 10 kb of recombinant DNA, including the regulatory elements required for independent gene regulation. These vectors transiently infect cells and are used in expression-targeted cancer therapy (Li *et al*, 2005; Small *et al*, 2006; Dorer and Nettelbeck, 2009).

Stable infection, often required for gene therapy, can be achieved with retroviral vectors such as lentiviruses. However, retroviral vectors with three independently regulated genes are not available to-date. Therefore, DPI delivery would require further optimization of the available retroviral vectors. For example, self-inactivating retroviral vectors (SIN), in which one of the LTRs is modified to inactivate its transcription initiation activity were developed to allow the expression of one independently regulated gene (Yu *et al*, 1986; Yee *et al*, 1987; Naviaux *et al*, 1996; Miyoshi *et al*, 1998; Mitta *et al*, 2002). As a further step toward retroviral delivery, lentiviral-based vectors, in which two transgenes are regulated by their own independent promoters, were already described (Yu *et al*, 2003; Semple-Rowland *et al*, 2007; Tian and Andreadis, 2009), suggesting that, with further optimization, lentiviral vectors such as required for DPI delivery could be developed.

## Materials and methods

### Cell culture

HEK-293T human kidney fibroblasts, HCT116+/+ and HCT116−/− human colorectal tumor cells, together with WI38-T/Neo and WI38-T3 human embryonic lung fibroblasts were kindly provided by Professor Varda Rotter (WIS). HEK-293T cells were grown in Dulbecco's modified Eagle's medium supplemented with 10% fetal calf serum (FCS), 2 mM L-glutamine, and antibiotics. WI-38 cells were grown in minimal essential medium (MEM) supplemented with 10% FCS, 1 mM sodium pyruvate, 2 mM L-glutamine, and antibiotics. HCT116 cells were grown in McCoy's Medium supplemented with 10% FCS, 2 mM L-glutamine, and antibiotics.

### Reagents

BVDU (Sigma B9647) was dissolved in DDW to stocks of 1 μg/μl, and was used at a final concentration of 10 μg/ml. GCV: (Roche, purchased as the drug Cymevene) was dissolved in DDW to stocks of 50 μg/μl, and was used at a final concentration of 100 μg/ml. Crystal violet (CV) staining solution: the staining solution consisted of 1 g CV powder (Sigma C3886), 25 ml EtOH 99%, 225 ml DDW.

### DNA delivery

Cells were plated in six-well plates 48 h before transfection, at initial cells densities of (1) $10^4$ WI38 cells/well, (2) $2.5 \times 10^5$ HCT116 cells/well, and (3) $2.5 \times 10^5$ HEK-293T cells/well for luciferase assays, or (3) $10^4$ WI38 cells/well, and (4) $5 \times 10^3$ 293T cells/well for viability assays. Transfections were performed with FuGENE-HD transfection reagent (Roche, 04-709-691-001) according to the manufacturer's protocol, with DNA/reagent ratios of 2:7 for the luciferase assay, and 1.7:6 for the cell viability assay, diluted in 100 μl reduced serum medium (Opti-MEM, GIBCO 31985-047).

### Plasmids

All plasmid maps are detailed in the Supplementary information section.

#### Plasmid pPromoter-1

The fusion protein DocS/VP16-AD is regulated by a human promoter of interest ('Promoter'). The plasmid is comprised of three modular

cassettes: (1) The promoter, which regulates the fusion protein; (2) the DocS gene; and (3) the optional PEST sequence. The optional PEST sequence is located downstream to the DocS gene. It consists of amino acids 422–461 of the mouse ornithine decarboxylase gene, which significantly reduces the lifetime of proteins fused to it (Evan and Littlewood, 1998). Translation of the PEST peptide requires cloning of the DocS/AD fusion gene in-frame to the PEST sequence. To exclude the PEST sequence from the fusion protein, the DocS sequence is cloned with a downstream STOP codon. The same plasmids, in which wild-type DocS was replaced with either *DocS15* or *DocS102*, were used for experiments with mutant DocS.

### Plasmid pPromoter-2
The fusion protein Coh2/GAL4–BD is regulated by a duplicate of a human promoter of interest ('Promoter'). Similarly to plasmid 1, plasmid 2 also has three modular cassettes: (1) the promoter, which regulates the fusion protein; (2) the Coh2 gene; and (3) the optional PEST sequence.

### pG5-luc
Expression of firefly luciferase is regulated by the yeast GAL4 promoter. The luciferase gene is flanked by unique restriction sites, which enable a simple replacement of the gene.

### pG5-TK1
This plasmid is identical to pG5-luc, except with TK1 in place of the luciferase gene.

### Plasmid pPromoter-5
The firefly luciferase is regulated directly by a human promoter of interest ('Promoter'), which was used to calibrate the input levels of each human promoter. The plasmid has three modular cassettes: (1) The promoter region, (2) the luciferase gene, and (3) an optional PEST sequence.

### Plasmid pPromoter-6
This plasmid, which is identical to plasmid 5, except for TK1 in place of luciferase, was used to study the effect of the killer gene TK1 on cell growth when it is regulated by a single promoter

- Plasmids pPromoter-1 + pPromoter-2 (input plasmids) and pG5-luc (output module plasmid) comprise the DPI with luciferase output.
- Plasmids pPromoter-1 + pPromoter-2 (input plasmids) and pG5-TK1 (output plasmid) comprise the DPI with TK1 output.

## Luciferase assays
The mixtures of plasmids, used at a total of 2 μg DNA/sample, are detailed in Supplementary Tables S1 and S2. Empty circular pGEM-t-Easy plasmid (Promega A3600) was used as non-specific DNA when needed, to complete the total DNA to 2 μg DNA/sample. Cells were collected, 48 h following transfection, centrifuged, and washed with 1 ml PBS in a 1.5-ml Eppendorf tube. The washed pellet was lysed with 50 μl lysis buffer (Promega E194A), and both firefly and renilla luciferase activity levels were measured in a 50 μl aliquot with Promega Dual-Luciferase® Reporter Assay kit (Promega E1980), in a Victor 1420 multi-label reader (Perkin-Elmer), according to the manufacturer's protocol. Transfection efficiency in each sample was estimated according to the activity levels of renilla luciferase, which was expressed from the plasmid pLXSN-Renilla, regulated by the stable viral LXSN promoter.

## Cell viability assays
Before plating, six-well plates were coated with poly-L-lysine-hydrobromide (Sigma P1274) to improve cell adhesion. The mixtures of plasmids, used at a total of 1.7 μg DNA/sample, are detailed in Supplementary Tables S3 and S4. Empty pGEM-t-Easy plasmid (Promega A3600) was used as non-specific DNA when needed, to complete the total DNA content to 1.7 μg DNA/sample. Cells were grown 48 h following transfection in the absence of BVDU/GCV, and total GFP expression (generated by the pCMV-GFP plasmid, in which GFP expression is regulated by the potent viral CMV promoter) in each well was measured at 200 μM resolution in the Typhoon 9400 fluorescence scanner (Amersham). This initial measurement of untreated cells was used to estimate the overall transfection efficiency for each sample (Supplementary Figure S2). At this point, the cells were observed under a fluorescence microscope to determine the percent of GFP-positive cells in the culture, to estimate the percent of transfected cells. Soon after the GFP measurement was performed, cells were incubated in the presence of either 10 μg/ml BVDU (for HEK-293T) or 100 μg/ml GCV (WI38-T/Neo and WI38-T3) to activate TK1 cytotoxicity. CV staining: Cells were incubated for 10 days in the presence of BVDU/GCV. Following treatment, cells were washed with 2 ml PBS, incubated for 15 min with 1 ml CV solution, and washed $\times 2$ with 2 ml DDW. Plates were dried and scanned with a Canon 5200 image scanner for qualitative analysis of cell density. To quantify cell densities, the CV stain immobilized in each sample was dissolved in 1 ml of 10% acetic acid/well. Next, 100 μl aliquots were transferred to 96-well plates and measured at $OD_{590}$ in the Synergy™ HT Multi-Mode Microplate Reader. Data normalization: To compare the effect of integrator expression on cell growth between the cell lines, the data had to be corrected for two important factors that affect final cell density: The cytotoxic effect of the transfection process, which varies between the cell lines and the different proliferation rates of the cell lines. Therefore, for each cell line, cell density ($CV_S$) was normalized according to the final density of a negative control sample ($CV_{NC}$), in which the output of the expression integrator was the luciferase gene instead of TK1, and which was defined as 0% cell death. Data are shown as percent cell death, which was calculated as: $\text{Cell death}\,[\%] = 100 - (\frac{CV_S}{CV_{NC}} \times 100)$, where $CV_S$ is the $OD_{590}$ absorbance of the dissolved CV in each sample, and $CV_{NC}$ is the $OD_{590}$ absorbance of the dissolved CV of the negative control sample.

## Supplementary information
Supplementary information is available at the *Molecular Systems Biology* website (www.nature.com/msb).

# Acknowledgements
We thank N Goldfinger, Y Buganim, H Besserglick, and V Rotter for their experimental support with the cell culture; and Y Atsmon, E Barda-Jaoui, and J Abadi for additional help. We thank E Bayer, A Karpol, N Barkai, A Bershadsky, E Braun, E Moses, M Oren, Y Pilpel, Y Shaul, and T Tlusty for comments and discussions; and S Schwarzbaum for a critical reading of the manuscript. We thank Adina Binder for her assistance. This work was supported by the Israel Science Foundation, the Minerva Foundation, and the Gurwin Fund.

*Author contributions*: This study was conceived by LN and RBZ. Experimental work was performed by LN. Analyses were performed by LN and RBZ. LN and RBZ wrote the paper.

# Conflict of interest
The authors declare that they have no conflict of interest.

# References
Anderson JC, Voigt CA, Arkin AP (2007) Environmental signal integration by a modular AND gate. *Mol Systems Biol* **3:** 133

Barak Y, Handelsman T, Nakar D, Mechaly A, Lamed R, Shoham Y, Bayer EA (2005) Matching fusion protein systems for affinity analysis of two interacting families of proteins: the cohesin-dockerin interaction. *J Mol Recognit* **18:** 491–501

Betzi S, Restouin A, Opi S, Arold ST, Parrot I, Guerlesquin F, Morelli X, Collette Y (2007) Protein-protein interaction inhibition (2P2I) combining high throughput and virtual screening: application to the HIV-1 Nef protein. *Proc Natl Acad Sci USA* **104:** 19256–19261

Bi WL, Parysek LM, Warnick R, Stambrook PJ (1993) *In-vitro* evidence that metabolic cooperation is responsible for the bystander effect observed with Hsv Tk retroviral gene-therapy. *Hum Gene Ther* **4:** 725–731

Boon K, Caron HN, van Asperen R, Valentijn L, Hermus MC, van Sluis P, Roobeek I, Weis I, Voute PA, Schwab M, Versteeg R (2001) N-myc enhances the expression of a large set of genes functioning in ribosome biogenesis and protein synthesis. *EMBO J* **20:** 1383–1393

Buganim Y, Solomon H, Rais Y, Kistner D, Nachmany I, Brait M, Madar S, Goldstein I, Kalo E, Adam N, Gordin M, Rivlin N, Kogan I, Brosh R, Sefadia-Elad G, Goldfinger N, Sidransky D, Kloog Y, Rotter V (2010) p53 regulates the Ras circuit to inhibit the expression of a cancer-related gene signature by various molecular pathways. *Cancer Res* **70:** 2274–2284

Callura JM, Dwyer DJ, Isaacs FJ, Cantor CR, Collins JJ (2010) Tracking, tuning, and terminating microbial physiology using synthetic riboregulators. *Proc Natl Acad Sci USA* **107:** 15898–15903

Caraglia M, Budillon A, Vitale G, Lupoli G, Tagliaferri P, Abbruzzese A (2000) Modulation of molecular mechanisms involved in protein synthesis machinery as a new tool for the control of cell proliferation. *Eur J Biochem* **267:** 3919–3936

Dachs GU, Dougherty GJ, Stratford IJ, Chaplin DJ (1997) Targeting gene therapy to cancer: a review. *Oncol Res* **9:** 313–325

Deans TL, Cantor CR, Collins JJ (2007) A tunable genetic switch based on RNAi and repressor proteins for regulating gene expression in mammalian cells. *Cell* **130:** 363–372

Dong ZH, Nor JE (2009) Transcriptional targeting of tumor endothelial cells for gene therapy. *Adv Drug Deliv Rev* **61:** 542–553

Dorer DE, Nettelbeck DM (2009) Targeting cancer by transcriptional control in cancer gene therapy and viral oncolysis. *Adv Drug Deliv Rev* **61:** 554–571

Evan G, Littlewood T (1998) A matter of life and cell death. *Science* **281:** 1317–1322

Gure AO, Tureci O, Sahin U, Tsang S, Scanlan MJ, Jager E, Knuth A, Pfreundschuh M, Old LJ, Chen YT (1997) SSX: a multigene family with several members transcribed in normal testis and human cancer. *Int J Cancer* **72:** 965–971

Harrington EA, Bennett MR, Fanidi A, Evan GI (1994) C-Myc-induced apoptosis in fibroblasts is inhibited by specific cytokines. *EMBO J* **13:** 3286–3295

Heldin CH (1995) Dimerization of cell-surface receptors in signal-transduction. *Cell* **80:** 213–223

Hernandez J, Thompson IM (2004) Prostate-specific antigen: a review of the validation of the most commonly used cancer biomarker. *Cancer* **101:** 894–904

Hoffmann A, Natoli G, Ghosh G (2006) Transcriptional regulation via the NF-kappa B signaling module. *Oncogene* **25:** 6706–6716

Hopfield JJ (1974) Kinetic proofreading—new mechanism for reducing errors in biosynthetic processes requiring high specificity. *Proc Natl Acad Sci USA* **71:** 4135–4139

Jerome V, Muller R (1998) Tissue-specific, cell cycle-regulated chimeric transcription factors for the targeting of gene expression to tumor cells. *Hum Gene Ther* **9:** 2653–2659

Jerome V, Muller R (2001) A synthetic leucine zipper-based dimerization system for combining multiple promoter specificities. *Gene Therapy* **8:** 725–729

Karpol A, Barak Y, Lamed R, Shoham Y, Bayer EA (2008) Functional asymmetry in cohesin binding belies inherent symmetry of the dockerin module: insight into cellulosome assembly revealed by systematic mutagenesis. *Biochem J* **410:** 331–338

Kim DK, Dzau VJ, Pratt RE (1993) Phenotypic regulation of H19 gene-expression in neointimal vascular smooth-muscle cells. *Circulation* **88:** 323

Leisner M, Bleris L, Lohmueller J, Xie Z, Benenson Y (2010) Rationally designed logic integration of regulatory signals in mammalian cells. *Nat Nanotechnol* **5:** 666–670

Li XQ, Zhao XN, Fang Y, Jiang X, Duong T, Fan C, Huang CC, Kain SR (1998) Generation of destabilized green fluorescent protein transcription reporter. *J Biol Chem* **273:** 34970–34975

Li YH, Idamakanti N, Arroyo T, Thorne S, Reid T, Nichols S, VanRoey M, Colbern G, Nguyen N, Tam O, Working P, Yu DC (2005) Dual promoter-controlled oncolytic adenovirus CG5757 has strong tumor selectivity and significant antitumor efficacy in preclinical models. *Clin Cancer Res* **11:** 8845–8855

Lim WA (2010) Designing customized cell signalling circuits. *Nat Rev Mol Cell Biol* **11:** 393–403

Liu T, Laurell C, Selivanova G, Lundeberg J, Nilsson P, Wiman KG (2007) Hypoxia induces p53-dependent transactivation and Fas/CD95-dependent apoptosis. *Cell Death Differ* **14:** 411–421

Mebratu Y, Tesfaigzi Y (2009) How ERK1/2 activation controls cell proliferation and cell death is subcellular localization the answer? *Cell Cycle* **8:** 1168–1175

Milyavsky M, Shats I, Erez N, Tang XH, Senderovich S, Meerson A, Tabach Y, Goldfinger N, Ginsberg D, Harris CC, Rotter V (2003) Prolonged culture of telomerase-immortalized human fibroblasts leads to a premalignant phenotype. *Cancer Res* **63:** 7147–7157

Milyavsky M, Tabach Y, Shats I, Erez N, Cohen Y, Tang XH, Kalis M, Kogan I, Buganim Y, Goldfinger N, Ginsberg D, Harris CC, Domany E, Rotter V (2005) Transcriptional programs following genetic alterations in p53, INK4A, and H-Ras genes along defined stages of malignant transformation. *Cancer Res* **65:** 4530–4543

Mitta B, Rimann M, Ehrengruber MU, Ehrbar M, Djonov V, Kelm J, Fussenegger M (2002) Advanced modular self-inactivating lentiviral expression vectors for multigene interventions in mammalian cells and *in vivo* transduction. *Nucleic Acids Res* **30:** e113

Miyoshi H, Blomer U, Takahashi M, Gage FH, Verma IM (1998) Development of a self-inactivating lentivirus vector. *J Virol* **72:** 8150–8157

Morgan DO (1997) Cyclin-dependent kinases: engines, clocks, and microprocessors. *Ann Rev Cell Develop Biol* **13:** 261–291

Naviaux RK, Costanzi E, Haas M, Verma IM (1996) The pCL vector system: rapid production of helper-free, high-titer, recombinant retroviruses. *J Virol* **70:** 5701–5705

Nettelbeck DM (2008) Cellular genetic tools to control oncolytic adenoviruses for virotherapy of cancer. *J Mol Med* **86:** 363–377

Nissim L, Beatus T, Bar-Ziv R (2007) An autonomous system for identifying and governing a cell's state in yeast. *Phys Biol* **4:** 154–163

Ohana P, Gofrit O, Ayesh S, Hochberg A (2004) Regulatory sequences of the H19 gene in DNA based therapy of bladder cancer. *Gene Ther Mol Biol* **8:** 181–192

Patil R, Chavez JB, Yee D (2000) Inducible expression of herpes simplex virus thymidine kinase increases sensitivity to ganciclovir but does not enhance bystander effect in breast cancer cells. *Breast Cancer Res Treat* **62:** 109–115

Peng W, Chen J, Huang YH, Sawicki JA (2005) Tightly-regulated suicide gene expression kills PSA-expressing prostate tumor cells. *Gene Therapy* **12:** 1573–1580

Ptashne M (1988) How eukaryotic transcriptional activators work. *Nature* **335:** 683–689

Rogakou EP, Pilch DR, Orr AH, Ivanova VS, Bonner WM (1998) DNA double-stranded breaks induce histone H2AX phosphorylation on serine 139. *J Biol Chem* **273:** 5858–5868

Ryan PC, Jakubczak JL, Stewart DA, Hawkins LK, Cheng C, Clarke LM, Ganesh S, Hay C, Huang Y, Kaloss M, Marinov A, Phipps SS, Reddy PS, Shirley PS, Skripchenko Y, Xu L, Yang JP, Forry-Schaudies S, Hallenbeck PL (2004) Antitumor efficacy and tumor-selective replication with a single intravenous injection of OAS403, an oncolytic adenovirus dependent on two prevalent alterations in human cancer. *Cancer Gene Therapy* **11:** 555–569

Semple-Rowland SL, Eccles KS, Humberstone EJ (2007) Targeted expression of two proteins in neural retina using self-inactivating, insulated lentiviral vectors carrying two internal independent promoters. *Mol Vision* **13:** 2001–2011

Small EJ, Carducci MA, Burke JM, Rodriguez R, Fong L, van Ummersen L, Yu DC, Aimi J, Ando D, Working P, Kirn D, Wilding

G (2006) A phase I trial of intravenous CG7870, a replication-selective, prostate-specific antigen-targeted oncolytic adenovirus, for the treatment of hormone-refractory, metastatic prostate cancer. *Mol Therapy* **14:** 107–117

Tabach Y, Milyavsky M, Shats I, Brosh R, Zuk O, Yitzhaky A, Mantovani R, Domany E, Rotter V, Pilpel Y (2005) The promoters of human cell cycle genes integrate signals from two tumor suppressive pathways during cellular transformation. *Mol Syst Biol* **1:** 2005.0022

Tian J, Andreadis ST (2009) Independent and high-level dual-gene expression in adult stem-progenitor cells from a single lentiviral vector. *Gene Therapy* **16:** 874–884

Tigges M, Fussenegger M (2009) Recent advances in mammalian synthetic biology-design of synthetic transgene control networks. *Curr Opin Biotechnol* **20:** 449–460

Touraine RL, Ishii-Morita H, Ramsey WJ, Blaese RM (1998) The bystander effect in the HSVtk/ganciclovir system and its relationship to gap junctional communication. *Gene Therapy* **5:** 1705–1711

Wang DZ, Wang HB, Brown J, Daikoku T, Ning W, Shi Q, Richmond A, Strieter R, Dey SK, DuBois RN (2006) CXCL1 induced by prostaglandin E-2 promotes angiogenesis in colorectal cancer. *J Exp Med* **203:** 941–951

Wera S, Degreve B, Balzarini J, De Clercq E, Thevelein JM, Neyts J (1999) Budding yeast as a screening tool for discovery of nucleoside analogs for use in HSV-1 TK suicide-gene therapy. *Biotechniques* **27:** 772–777

Yamaizumi M, Mekada E, Uchida T, Okada Y (1978) One molecule of diphtheria-toxin fragment a introduced into a cell can kill cell. *Cell* **15:** 245–250

Yee JK, Moores JC, Jolly DJ, Wolff JA, Respess JG, Friedmann T (1987) Gene-expression from transcriptionally disabled retroviral vectors. *Proc Natl Acad Sci USA* **84:** 5197–5201

Yu SF, Vonruden T, Kantoff PW, Garber C, Seiberg M, Ruther U, Anderson WF, Wagner EF, Gilboa E (1986) Self-inactivating retroviral vectors designed for transfer of whole genes into mammalian-cells. *Proc Natl Acad Sci USA* **83:** 3194–3198

Yu XB, Zhan XC, D'Costa J, Tanavde VM, Ye ZH, Peng T, Malehorn MT, Yang XM, Civin CI, Cheng LZ (2003) Lentiviral vectors with two independent internal promoters transfer high-level expression of multiple transgenes to human hematopoietic stem-progenitor cells. *Mol Therapy* **7:** 827–838

Zhang WS, Purchio AF, Chen K, Wu JM, Lu L, Coffee R, Contag PR, West DB (2003) A transgenic mouse model with a luciferase reporter for studying *in vivo* transcriptional regulation of the human CYP3A4 gene. *Drug Metab Disposit* **31:** 1054–1064

Real data.
Real installations.
Real super-resolution imaging.


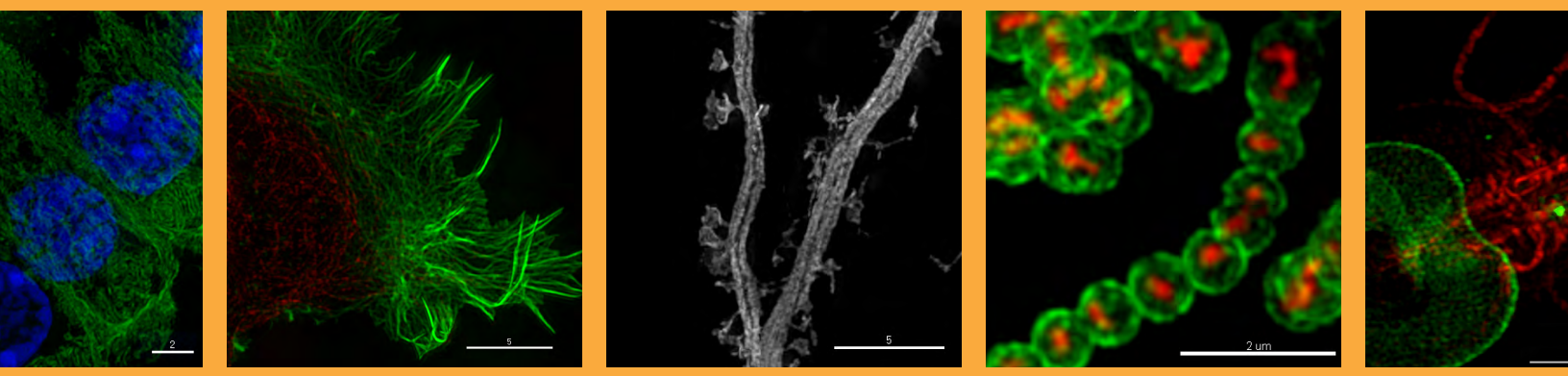


Learn more about the DeltaVision OMX super-resolution imaging system at **www.superresolution.com**.

applied precision

1040 12th Ave NW | Issaquah, WA 98027